J Mater Sci (2023) 58:11044–11061

Composites & nanocomposites

A robust copper mesh-based superhydrophilic/superoleophobic composite for high-flux oil–water separation

Ruhui Li[1], Ruobing Yu[1,*], Junhan Fan[1], and Bu Chang[2]

[1] School of Materials Science and Engineering, East China University of Science and Technology, Shanghai 200237, People's Republic of China

[2] Science and Technology Committee of Inner Mongolia Aerospace Hongxia Chemical Co., Hohhot 010010, People's Republic of China

Received: 7 May 2023
Accepted: 20 June 2023
Published online: 5 July 2023

ABSTRACT

With the fast growing of oily contaminants, continuous oil/water separation with high flux is in demand. Superhydrophilic/superoleophobic composites are considered as ideal candidates. In this work, the oil–water separation composite is from superhydrophilic copper mesh coated by robust superhydrophilic/superoleophobic paint based on fluorine-containing epoxy resin. Firstly, a superhydrophilic/superoleophobic coating with excellent comprehensive properties was prepared through hydrophilic epoxy and superhydrophilic/superoleophobic TiO_2. Then copper mesh was treated into being superhydrophilic, and the superhydrophilic/superoleophobic coating was sprayed on the superhydrophilic copper mesh to obtain oil–water separation material. As a result, the oil–water separation efficiency of the separation material is higher than 99.7%, the water flux is higher than 80,000 L m^{-2} h^{-1}, and it has excellent mechanical properties. The oil–water separation material is promising for the applications.

Introduction

With the development of economy and a large number of oil utilization, a large amount of oily wastewater is generated [1]. If it is not handled properly or directly discharged, it will have an irreversible impact on the ecological environment [2]. Traditional oil–water separation methods include flocculation method [3], centrifugation method, air flotation method [4], etc. These methods have disadvantages such as low separation efficiency, high cost, and poor recovery rate. The development of oil–water separation materials with special wettability is of great significance for building an environment-friendly society [5, 6]. In order to remove oil in water, filtration materials can be divided into two

Handling Editor: Stephen Eichhorn.

Address correspondence to E-mail: rbyu@ecust.edu.cn

https://doi.org/10.1007/s10853-023-08711-0

categories, oil-removing material (superoleophilic/superhydrophobic material) and water-removing material (superhydrophilic material or superhydrophilic/superoleophobic material).

At present, "oil-removing" superoleophilic/superhydrophobic materials have been developed [7–9]. For above "oil-removing" wetting materials, oil is easily sticked on the surface and block the pores of the wetting material, resulting in low efficiency of oil–water separation [10, 11]. So far, superhydrophilic surfaces have attracted much attention in oil–water separation. Superhydrophilic surfaces exhibit underwater superoleophobicity and can be used as oil–water separation materials. Matsubayashi et al. [12] have prepared a calcium alginate hydrogel (Ca–Alg), which exhibits superhydrophilicity in air and superoleophobicity in water, and can achieve oil–water separation with high efficiency (above 99.5%) and high speed (the water flux was as high as 46,979 L m^{-2} h^{-1}). Yang et al. [13] prepared a three-dimensional porous Ni–Co–LDH (layered double hydroxide) nanomembrane by solvothermal method, which was used for the separation of oil/water mixtures and oil-in-water emulsions. The separation efficiency is about 99.5%, and the water flux is higher than 70,000 L m^{-2} h^{-1}. Wang et al. [14] used chitosan and dopamine to prepare a composite hydrogel with a rough surface on the surface of cotton fabric, which was characteristic of superhydrophilicity and underwater superoleophobicity, and the separation efficiency of various oil–water mixtures was higher than 99.5%. Ni et al. [15] deposited tannic acid and (3-aminopropyl) triethoxysilane on the surface of waste carbon fibers by a one-pot method to prepare a superhydrophilic/underwater superoleophobic membrane, which was able to separate surfactant-stabilized oil-in-water emulsions. The water flux is as high as 713 L m^{-2} h^{-1}, and the separation efficiency is up to 99.8%. Qu et al. [16] have used montmorillonite, β-cyclodextrin, tannic acid, and sodium alginate to prepare a suspension, and then prepared a superhydrophilic underwater superoleophobic PVDF membrane by a simple suction filtration method, whose separation efficiency for various surfactant-stabilized oil-in-water emulsions and oil–water mixtures is up to 99.6% and 95%, respectively. Also, it can effectively adsorb organic dyes and heavy metal ions. Zhou et al. [17] prepared superhydrophilic/underwater superoleophobic cotton fabrics by depositing gallic acid (GA) on polyethyleneimine (PEI), followed by complexation with Cu^{2+}. The water contact angle is 0°, and the underwater oil contact angle is 162.2 ± 2.4°. In the case of separation of surfactant-stabilized oil–water emulsions, the efficiency is above 99.1%. Zeng et al. [18] treated the stainless steel wire mesh soaked in magnesium nitrate solution at high temperature to prepare a superhydrophilic/underwater superoleophobic stainless steel wire mesh with a coral-like structure. The oil–water separation efficiency reaches 99.0%, the flux is 6195 L m^{-2} h^{-1}, and after using 10 times, and the oil–water separation efficiency is always as high as 98.0%.

Although superhydrophilic material is able to separate oil from water, the material can be contaminated by oil when it is not wetted by water, and in the process of oil–water separation, the repellency to oil is weak, resulting in low separation efficiency. In recent years, "water-removing" superhydrophilic/superoleophobic materials are superior to superhydrophilic materials, and can meet the need of oil–water separation. This kind of material repels oil and allows water to pass through easily, which can avoid clogging by high-viscosity oil. Some superhydrophilic/superoleophobic materials have been prepared. Yang et al. [19, 20] first used polydiallyldimethylammonium chloride and sodium perfluorooctanoate to synthesize a hydrophilic and oleophobic polymer, and then added silica particles to prepare a coating by spraying. The contact angle of hexadecane on its coating reaches 155°, the coated stainless steel mesh can repeat oil–water separation under the action of gravity, and the separation efficiency is above 99%. Li et al. [21] have prepared superhydrophilic/superoleophobic titanium dioxide (TiO_2) by grafting fluorosurfactant (FS-50) on the surface of TiO_2. The hydrophilic head of FS-50, combined with TiO_2, has a strong affinity for water, and the tail of the FS-50 fluorine chain shows oil repellency; a superhydrophilic/superoleophobic coating is prepared by spraying, which can separate oil–water mixtures and oil–water emulsions. The separation efficiency is higher than 98.5%, and the water flux is 600 L m^{-2} h^{-1}, which can also purify pollutants under the irradiation of ultraviolet light. Lu et al. [22] first synthesized sodium perfluorooctanoate, and then mixed it with titanium dioxide particles, bis(3(trimethoxysilyl)propyl)amine (BTMEPA) and (3-aminopropyl)triethoxysilane (APTES) to obtain the suspension for spraying. The fluorinated groups ($–CF_3$ and $–CF_2–$) in the coating have repellency to oils, and

components such as carboxyl groups, quaternary ammonium groups, and sodium ions have strong affinity for water, and the as-prepared coating is superhydrophilic/superoleophobic in both air and water. Also, copper mesh without treatment coated by above suspension can separate the mixture of oil and water with the separation flux of 2750 L/ (m^2 h bar).

At present, some wetting materials have been used to separate oil–water mixtures, but in the separation process, the separation materials can withstand a higher transmembrane pressure, which can provide higher liquid permeability and maintain a higher separation efficiency and long life span. Thus, there are higher requirements on the mechanical property of the separation material. Epoxy resins have excellent adhesion, chemical stability, and mechanical stability, and were often used to prepare super-wetting materials in the past. Researchers have prepared epoxy resins with wetting properties, which are used in oil–water separation materials. For example, Lu et al. [23] prepared a single-terminal isocyanate (NCO) polyurethane (PU) prepolymer with a polyethylene glycol hydrophilic chain segment and grafted it onto an epoxy resin (EP) molecular chain for hydrophilic modification of the epoxy resin; when the PU content is close to 70%, the water contact angle could reach 47.2°. Qian et al. [24] have modified epoxy resin with polyethylene glycol to obtain a hydrophilic epoxy resin; when the addition amount of polyethylene glycol was 20%, the water contact angle could reach 54°. Through the template method, a microstructure is constructed on the surface of the resin, and the water contact angle is 0° (being superhydrophilic). Ying et al. [25] synthesized a hydrophilic and oleophobic epoxy resin by the reaction from polyethylene glycol, Zonyl@FSN-100 fluorocarbon surfactant and epoxy resin. Compared with the original epoxy resin, water contact angle is reduced by nearly 30°, the contact angle of hexadecane is increased by 17°. Li et al. [26] prepared a superhydrophilic transparent epoxy coating by mixing epoxy resin, amine curing agent, and nonionic surfactant (Triton X-100) by one-step casting method, and the contact angle was less than 5°. The coating has excellent antifog performance, and the oil–water separation efficiency exceeds 96%.

From above, there are some disadvantages in superhydrophilic/superoleophobic coatings, such as low adhesive strength. For the oil–water materials based on superhydrophilic/superoleophobic coatings, the performance is not good enough so that there is much room to improve the oil–water separation materials. In the study, the superhydrophilic/superoleophobic coating with good comprehensive properties is in demand at first; in the next step, the aim is to prepare the oil–water separation material based the above coating. The durability and mechanical stability of wetting coatings were enhanced by the application of the strategy of "adhesive+particles." Here, a hydrophilic matrix material with strong adhesion (hydrophilic fluorine-containing epoxy) and superhydrophilic/superoleophobic titanium dioxide was chosen for the preparation of composite. The hydrophilic fluorine-containing epoxy is from epoxy monomer cured by the hydrophilic fluorine-containing curing agent, which is from perfluorooctanoic acid and curing agent (polyetheramine) through ionic interaction. At the same time, by the introduction of a large number of hydrophilic and oleophobic groups on the surface of the titanium dioxide particles, superhydrophilic/oleophobic titanium dioxide particles are formed. The coating from the mixture of hydrophilic/oleophobic fluorine-containing epoxy resin and superhydrophilic/superoleophobic titanium dioxide particles, is expected to be high adhesive strength, which is not reported.

In order to obtain the oil–water materials with good comprehensive properties, multiple structural combination is applied, including superhydrophilic copper mesh and superhydrophilic/superoleophobic coating with high adhesive strength (the coating was spraying on the superhydrophilic copper mesh), which is not reported. The oil–water separation material with good comprehensive properties is promising for the applications.

Materials and methods

Chemicals and materials

Epoxy resin (E51) was purchased from Shanghai Fanxiao Chemical Technology Co., Ltd. Bromocresol green indicator solution (99.7%), methylene blue (99.7%), and castor oil (99.7%) were purchased from Shanghai McLean Biochemical Technology Co., Ltd. Perfluorooctanoic acid (99.7%) (PFOA) and bis-(3-trimethoxysilylpropyl)amine (99.7%) were purchased from Shanghai Dibo Biotechnology Co., Ltd.

Polyetheramine (D400, 99.7%) was purchased from Changzhou Runxiang Chemical Co., Ltd. Titanium dioxide (0.2–0.4 μm) was purchased from Aladdin Biochemical Technology Co., Ltd. Ammonium persulfate (99.7%), sodium hydroxide (99.7%), ethylene glycol (99.7%), isopropanol (99.7%), ethanol (99.7%), and tetrahydrofuran (99.7%) were purchased from Shanghai Titan Technology Co., Ltd. Concentrated hydrochloric acid (content: 36–38%) was purchased from Sinopharm Chemical Reagent Co., Ltd. Soybean oil and sesame oil were purchased from Yihai Kerry Food Marketing Co., Ltd. The olive oil was purchased from Hangzhou Oriel Import and Export Trading Co., Ltd. Diesel (0 #) was purchased Shanghai Petrochemical Co., Ltd. Hexadecane (99.7%) was purchased from Shanghai Zhanyun Chemical Co., Ltd. Copper mesh (700 mesh) was purchased from Shanghai screen filter cloth manufacturers.

Preparation of fluorine-containing curing agent

PFOA (0–6 wt%), polyetheramine (D400), and tetrahydrofuran (20 wt%) were added into a flask with magnetically stirring until the solution became clear, and then the flask was heated up to 40 °C in an oil bath. Subsequently, the reaction was carried out in a closed environment for 0.5 h to obtain a fluorine-containing polyetheramine curing agent. The schematic diagram of the reaction is shown in Fig. 1.

Surface treatment of copper mesh

The 700-mesh copper mesh was ultrasonically cleaned with acetone and deionized water in turn, and soaked in a mixed aqueous solution of 2.5 M sodium hydroxide and 0.13 M ammonium persulfate for 0.5–20 min at room temperature. After the copper mesh was taken out of the above solution, it was rinsed with deionized water and was dried under nitrogen.

Preparation of superhydrophilic/superoleophobic coatings

Preparation of superhydrophilic/superoleophobic suspension is according to reference [27]: 0.1 mL of bis-(3-trimethoxysilylpropyl)amine and 0.1 mL of 3-aminopropyltriethoxysilane were added to 15 mL

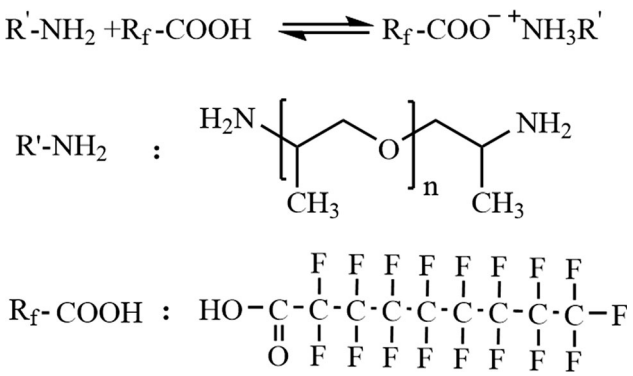

Figure 1 The schematic diagram for the preparation of fluorine-containing curing agent.

of ethanol with magnetically stirring to form a homogeneous solution, named as solution A. 0.5 g PFOA and 0.05 g sodium hydroxide (NaOH) were added to 15 mL of ethanol with magnetically stirring for 2 h to fully react to obtain a sodium perfluorooctanoic acid solution. Then 3 g of TiO_2 nanoparticles was ultrasonically dispersed in the ethanol solution of sodium perfluorooctanoic acid to form solution B, and solution A was added dropwise to solution B, mixed and stirred for 3 h.

Taking out the above superhydrophilic/superoleophobic suspension, 0 g, 1 g, 2 g, or 3 g of epoxy resin and corresponding mass of fluorine-containing curing agent were added into it, respectively. Subsequently, the mixtures were magnetically stirred for 15 min. The suspension was sprayed on the surface of the copper mesh with a compressed air of 0.3 MPa at the distance of 20 cm, and the spraying time was about 1 min. The sprayed copper mesh was cured in an oven at 100 °C for 2 h. The preparation process of the coating is shown in Fig. 2.

Characterization

The morphology of the copper mesh surface and the coating on the copper mesh were observed by field emission scanning electron microscope (SEM, S-4800, Hitachi Corporation, Japan), and the surface elements of the coating were characterized by X-ray energy dispersive spectrometer analysis (EDS, QUANTAX 400-30, Bruker AXS GmbH, Germany). During the test, the sample was adhered by the use of the conductive adhesive, and the surface was sprayed with gold. At ambient temperature, the water contact angle (WCA) and oil contact angle (OCA) of the coating were measured by a contact angle tester

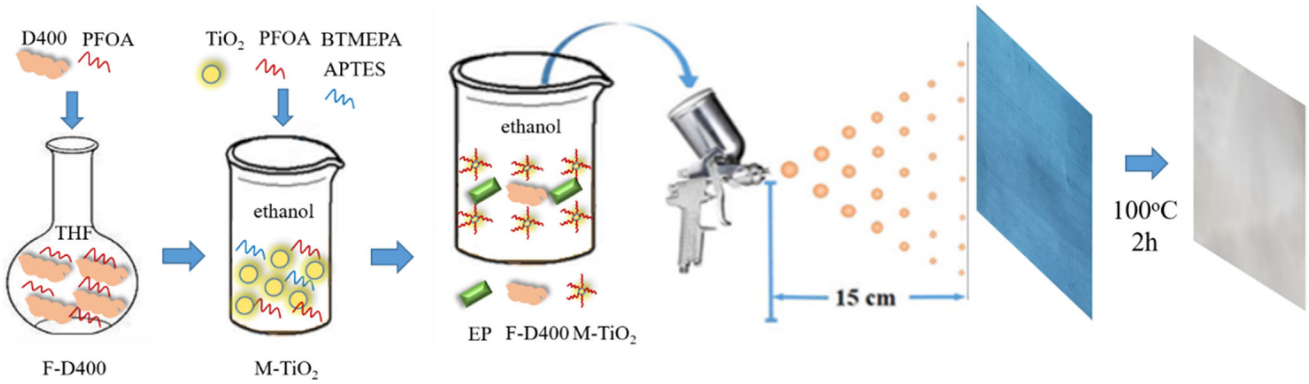

Figure 2 The preparation procedure for the oil–water separation material.

(JC2000D2, Shanghai Zhongchen Digital Technology Equipment Co., Ltd, China). Use a quantitative syringe to drop 5 μL deionized water drops or oil drops on the surface of the sample, take five different points on the surface of the sample for testing, and average the values to obtain the contact angle (CA). X-ray photoelectron spectroscopy (Thermo Scientific Escalab 250Xi, Massachusetts, MA, USA) and fourier transform infrared spectroscopy (Nicolet 6700, Thermo Fisher, Waltham, MA, USA) were used to analyze the elements and functional groups. The amine value of the fluorine-containing curing agent was determined by hydrochloric acid–ethanol titration (according to ASTM D2074-07). Firstly, 0.5 M hydrochloric acid-ethylene glycol-isopropanol solution was prepared. Accurately weigh about 3 g of the sample and place it in a 250 mL conical flask, add 50 mL of ethylene glycol and isopropanol as solvent (1:1 by volume), shake the flask continuously to dissolve the samples, add three drops of bromomethyl green indicator, and 0.5 M hydrochloric acid-ethylene glycol-isopropanol standard solution was used for titration, and turning point that the solution changed from blue to yellow was set as end point. Calculate the total amine value using formula (1).

$$\text{Total amine value} = \frac{\text{MV} \times 56.1}{\text{W}} \quad (1)$$

M: the concentration of the standard solution of hydrochloric acid; *V*: volume of consumed standard solution; *W*: the mass of the sample; *56.1*: the molecular weight of potassium hydroxide.

Separation of oil–water mixture

Select a copper mesh (700 mesh) coated with a superhydrophilic/superoleophobic coating to separate the oil–water mixture, which was placed in the middle of the separator, and clamp it with a clamp (see Fig. 13). Oil–water mixtures were including the mixture of soybean oil and water, diesel oil and water, castor oil and water, olive oil and water, hexadecane and water, sesame oil and water. Pour the oil–water mixture into the upper tube of the separation unit, with gravity as the only driving force. During the separation process, the water is collected after infiltrating the copper mesh, and the oil is excluded above the copper mesh. The separation efficiency η is calculated according to formula (2), and the water flux F is calculated by formula (3).

$$\eta = \frac{\text{m1}}{m} \times 100\% \quad (2)$$

where m, $m1$ are the mass of oil before and after the separation process.

$$F = \frac{V}{S \times t} \quad (3)$$

where V is the volume of permeated water; S is the effective area of the oil–water separation material, and the effective separation area is about 19.63 cm^2; t is the time required to complete the oil–water separation process.

Results and discussion

Structure and properties of fluorine-containing curing agent

Figure 3 is FT-IR spectrum of perfluorooctanoic acid, polyetheramine (D400), and fluorine-containing polyetheramine (F-D400). In the FT-IR spectrum of fluorine-containing polyetheramine, two absorption peaks at 1688 and 1456 cm^{-1}, correspond to the

vibration of the −C=O group of the amide I band; the absorption peaks located at 2673.8 and 2575.7 cm^{-1} belong to the symmetry of N^+H_3 primary ammonium salts and asymmetric stretching, indicating that polyetheramine (D400) has been transformed into the ammonium salt of polyetheramine [28].

The epoxy monomer was cured by fluorine-containing polyetheramine (F-D400) to prepare fluorine-containing epoxy resin (FEP). Figure 4c is the XPS total spectrum of fluorine-containing epoxy resin (FEP) with C, O, N, and F elements. According to the XPS data, the proportions of C, O, N, and F were 83.52%, 14.57%, 1.78%, and 0.14%, respectively. Figure 4a is a high-resolution C 1 s spectrum, and the peaks of C=O (289.00 eV), C–O (286.40 eV) and C–C (284.8 eV) can be detected. Figure 4b is the high-resolution spectrum of N 1 s, and there are two fitting peaks, assigning to the N^+H_3 primary ammonium salt (401.21 eV) and the NR_3 tertiary amine group (399.19 eV), indicating the formation of primary ammonium salt and tertiary amine groups on the surface of the sample, being contributable to the hydrophilicity.

The contact angles of FEP are shown in Table 1. The contact angle of fluorine-containing epoxy resin (FEP) is reduced with the increase in the PFOA, indicating that the hydrophilicity of epoxy resin was gradually enhanced. The contact angle of the original epoxy resin is 75.3°; with the addition of 3 wt% PFOA, the contact angle is down to 60.3°; when the addition amount of PFOA is above 3 wt%, the contact angle decreases more gently. With the further increase in the dosage of perfluorooctanoic acid, the water contact angle of FEP will not be greatly reduced, and the amino group of the polyetheramine will be consumed too much, which will affect the curing of the epoxy resin. At the same time, fluoro-containing long chain is helpful for the improvement of the superoleophobicity. Therefore, 5 wt% PFOA was chosen to modify D400 (the curing agent of epoxy resin) (The total amine value of F-D400 is 232.3 mg KOH/g, while that of the original D400 is between 220 and 273 mg KOH/g, so F-D400 did not affect the curing degree of the epoxy resin).

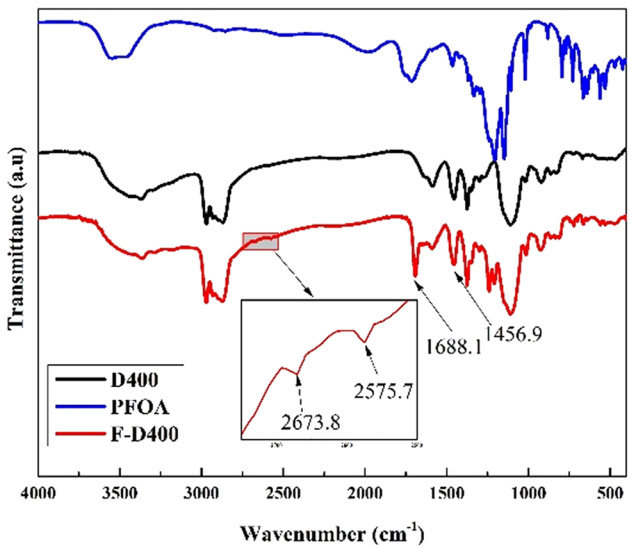

Figure 3 FT-IR spectra of perfluorooctanoic acid (PFOA), polyether amine (D400), and fluorine-containing polyetheramine (F-D400).

Structure and properties of fluorine-containing epoxy-based coatings

The structure of modified titanium dioxide

Figure 5 is FT-IR spectra of pristine titanium dioxide particles and modified titanium dioxide particles. In Fig. 5, the broad absorption peak at 3447 cm^{-1} is attributed to -OH on the surface of titanium dioxide, indicating that the original titanium dioxide is hydrophilic. For TiO_2 modified by bis-(3-trimethoxysilylpropyl)amine and PFOA, there are new absorption peaks at 1440 and 1370 cm^{-1}, corresponding to $–CF_3$ and $–CF_2–$ of PFOA, respectively [27]. The new absorption peaks at 1685 and 1562 cm^{-1} correspond to the −C=O group stretching vibration of the amide I band in the spectrum of modified titanium dioxide, which is the proof that PFOA was successfully grafted on the surface of TiO_2 [27]. The absorption peaks at 3421, 2915, and 2852 cm^{-1} are mainly associated with the N−H, $-CH_3$, and $-CH_2-$ groups of bis-(3-trimethoxysilylpropyl)amine [27].

Structure and properties of fluorine-containing epoxy-based coatings

The mass ratio of fluorine-containing epoxy resin (FEP) and modified titanium dioxide particles (set 3 g) in the suspension was set as 0:3, 1:3, 2:3, 3:3. The above suspensions were sprayed on the glass slides, respectively, and the coatings were obtained after drying (named as B1 (0:3, the blank sample), B2 (1:3), B3 (2:3), B4 (3:3), respectively). The wetting properties were evaluated by the spreading of water and

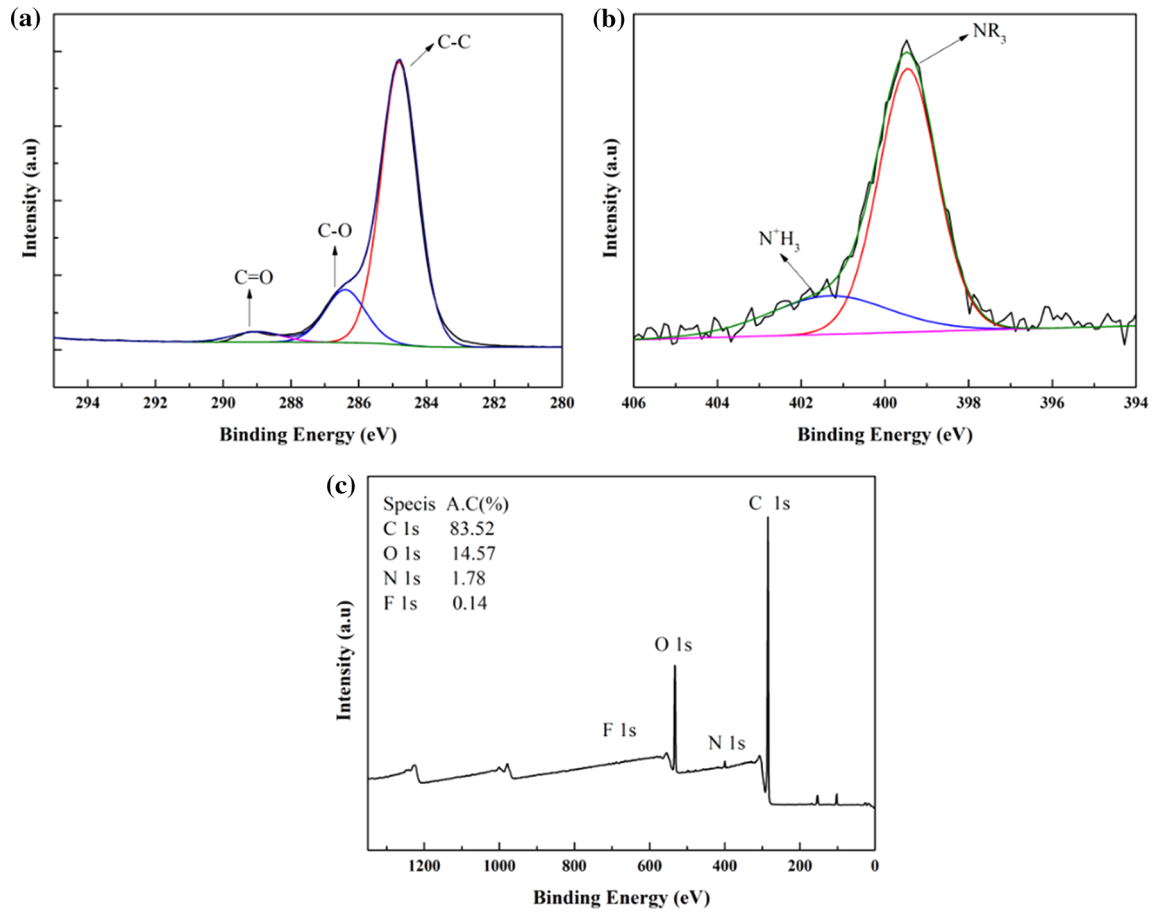

Figure 4 **a** High-resolution C 1 s spectrum, **b** high-resolution N 1 s spectrum, and **c** XPS total spectrum of the cured FEP.

Table 1 The effect of the content of perfluorooctanoic acid on the contact angle of

Content	0	1 wt%	2 wt%	3 wt%	4 wt%	5 wt%	6 wt%
WCA(°)	75.3 ± 1.5	67.0 ± 0.6	65.1 ± 1	60.3 ± 0.7	58.5 ± 0.5	57.4 ± 0.3	55.4 ± 0.4

low surface tension oils (including soybean oil, diesel oil, and hexadecane) on the coating surface. The results are shown in Fig. 6 and Table 2.

From Table 2, the contact angles of water, soybean oil, diesel oil, and hexadecane on the coating B1 are 0°, 152.3 ± 0.6°, 154.3 ± 1.5°, 142.1 ± 1.8°, respectively. The coating B1 is characteristic of superhydrophilicity and superoleophobicity, so it is believed that the modified titanium dioxide has superhydrophilicity and superoleophobicity, which is called superhydrophilic/superoleophobic titanium dioxide. When the mass ratio of fluorine-containing epoxy resin (FEP) (the mass is 1 g) and modified titanium dioxide particles is 1:3, the contact angles of water, soybean oil, diesel oil, and hexadecane on the coating B2 are 0°, 150.8 ± 0.7°, 151.6 ± 1.3°, 136.8 ± 0.9°. The contact angles of the coatings to oil are slightly reduced compared to those without the addition of fluorine-containing epoxy resin (FEP). When the mass ratio of fluorine-containing epoxy resin (FEP) and modified titanium dioxide particles is 2:3 and 3:3, respectively, the oleophobic angle of the coating is greatly reduced to about 80°. This is because the superhydrophilic/superoleophobic TiO_2 particles were encapsulated by fluorine-containing epoxy resin (FEP), and the fine rough coarse surface disappears.

The state of different liquid drops on coating B2 of the glass slide is shown in Fig. 6a. The water stained with methylene blue spreads rapidly on the surface of the coating, and soybean oil, hexadecane, and diesel are spherical on the surface of the coating,

which is superhydrophilic and superoleophobic in air. As shown in Fig. 6b, the silver mirror phenomenon occurs when the coating is immersed in soybean oil. This is because the surface is superoleophobic (there is an air layer between the droplet and the rough surface), and the light is reflected on the air layer, resulting in a mirror phenomenon. As shown in Fig. 6c–f, when coating was formed on the substrates (c) glass fiber cloth, (d) filter paper, (e) foam, (f) copper mesh, sesame oil, olive oil, castor oil, soybean oil drops were spherical, being superoleophobic.

SEM images of coating B1, B2, B3, and B4 were shown in Fig. 7. When no fluorine-containing epoxy resin (FEP) is added, as shown in Fig. 7a–b, the coating B1 is completely composed of particles, and the coating is flat. The particle size of titanium dioxide particles is about 0.2 um, and holes and protrusions with a about 1 um are formed by spraying and stacking. This micro-nanostructure makes the coating oleophobic. As the adhesion of the coating comes from the interaction between bis-(3-trimethoxysilylpropyl)amine and the hydroxyl groups on the surface of the substrate, the mechanical properties of the coating are poor and the coating is easy to be fallen off. When applied to the oil–water separation, it is

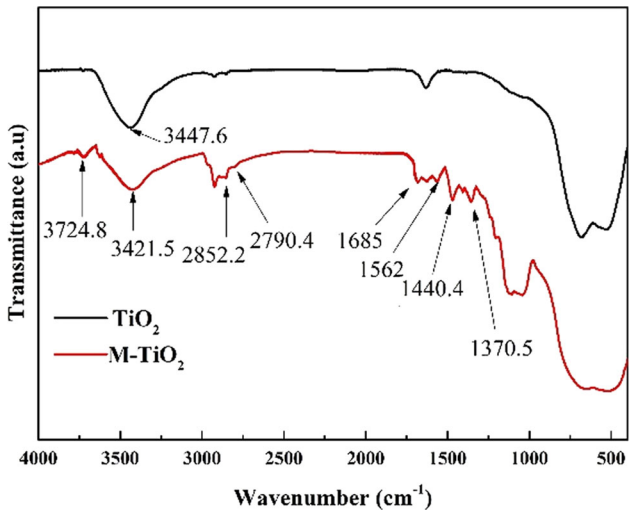

Figure 5 FT-IR spectra of original titanium dioxide and modified titanium dioxide.

Table 2 The contact angles of water and oil on coatings B1, B2, B3, and B4

CA (°)	Water	Soybean oil	Diesel oil	Hexadecane
B1	0	152.3 ± 0.6	154.3 ± 1.5	142.1 ± 1.8
B2	0	150.8 ± 0.7	151.6 ± 1.3	136.8 ± 0.9
B3	0	87.2 ± 1.2	74.0 ± 2.0	72.7 ± 1.7
B4	0	88.1 ± 1.5	74.4 ± 1.5	70.3 ± 0.9

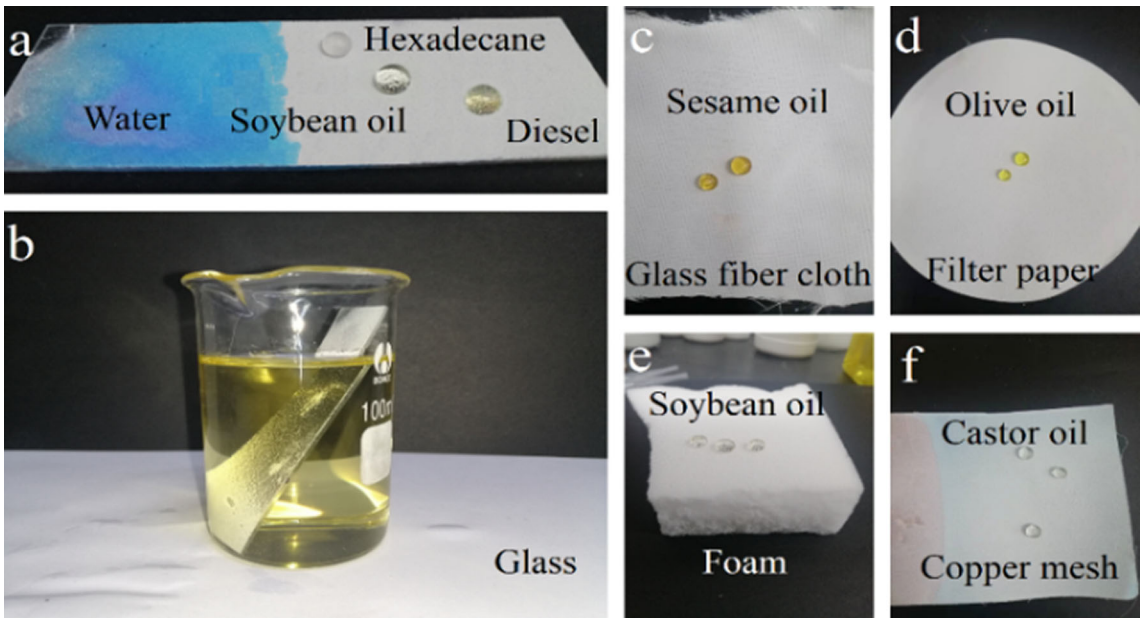

Figure 6 **a** The photograph of water and oil on coating B2 **b** silver mirror phenomenon of coating B2 in soybean oil, **c** and **f** different oils on the B2 coating of different substrate surfaces **c** glass fiber cloth, **d** filter paper, **e** foam, **f** copper mesh.

easy to lose superoleophobicity under the impact of water flow due to the broken coating.

When the mass ratio of fluorine-containing epoxy resin (FEP) and titanium dioxide particles is 1:3, as shown in Fig. 7c and d, a part of the titanium dioxide particles is covered by the fluorine-containing epoxy resin, and some of the titanium dioxide particles are bonded with fluorine-containing epoxy resin on the surface. The coating with numerous cavities can store air and be superoleophobic. At the same time, the oil contact angle of the coating is slightly lower than that without the addition of fluorine-containing epoxy

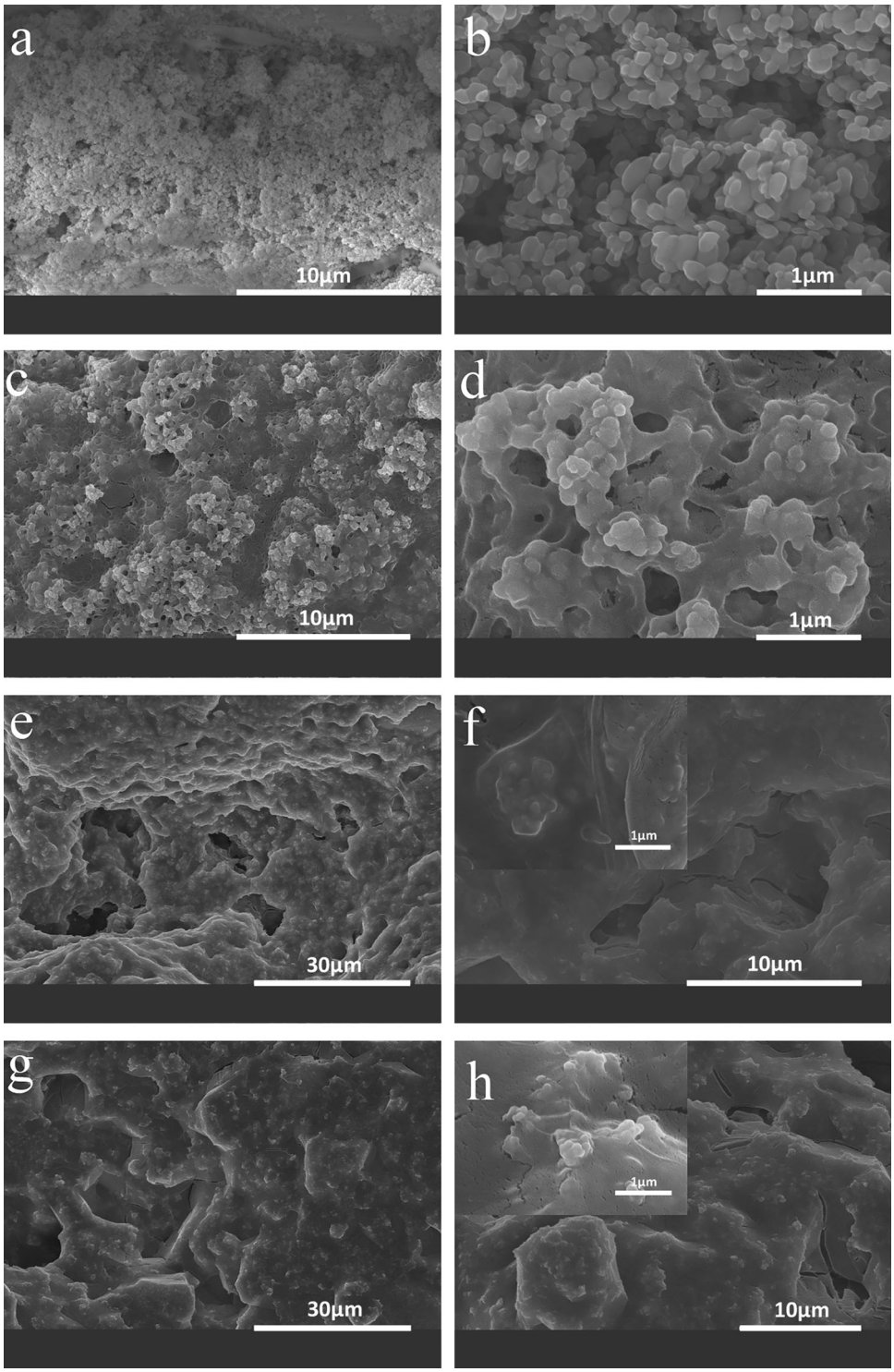

Figure 7 SEM images of coatings with the mass ratio of fluorine-containing epoxy resin (FEP) and modified titanium dioxide particles of 0: 3, 1: 3, 2: 3, and 3: 3, **a**-**b**, **c**-**d**, **e**-**f**, and **g**-**h** are coatings B1, B2, B3, and B4, respectively.

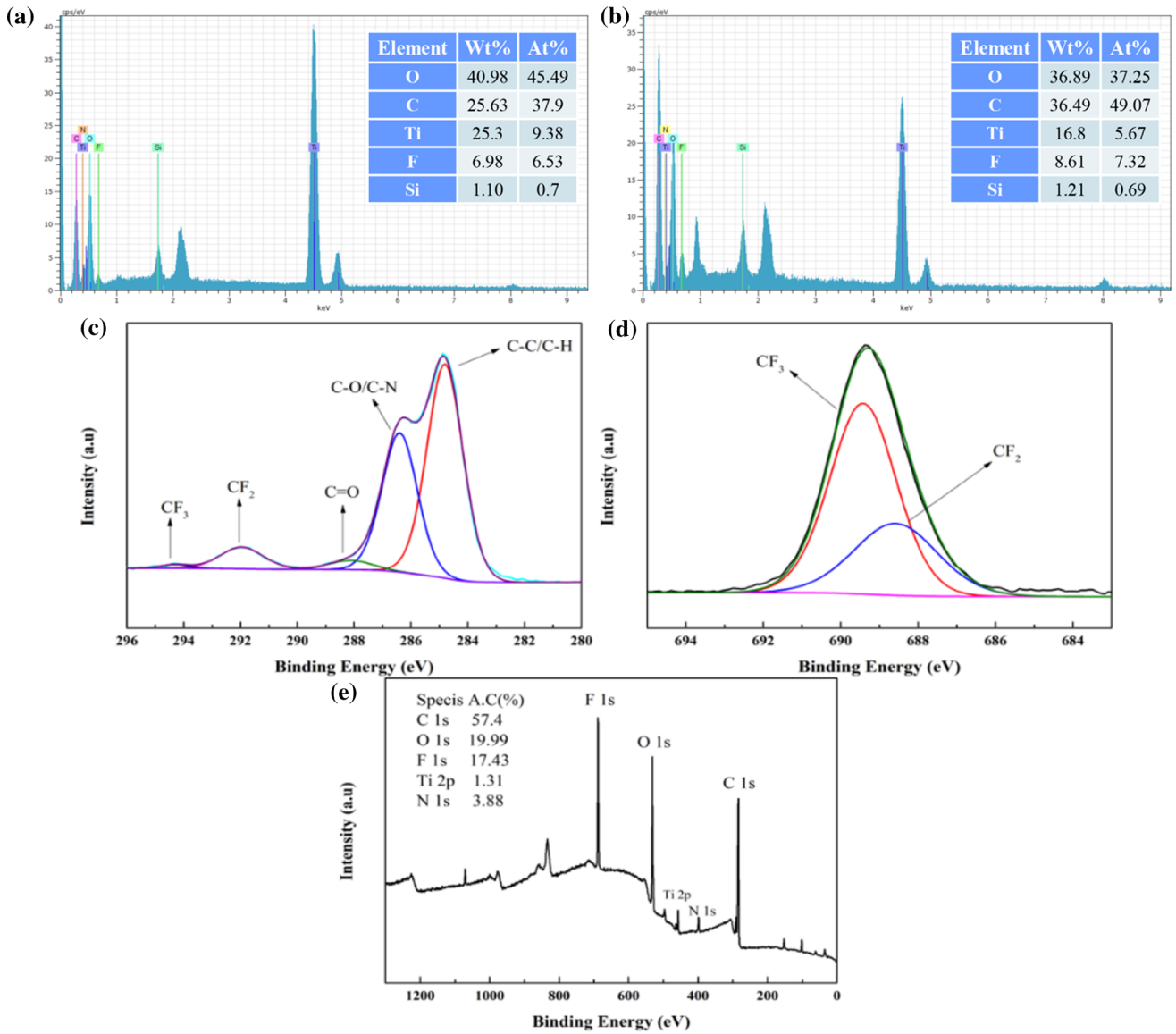

Figure 8 EDS mapping **a** curing with original D400, **b** curing with fluorine-containing D400, **c** high-resolution C 1 s spectrum, **d** high-resolution F 1 s spectrum, and **e** XPS total spectrum of B2 coating.

resin. This is because the oleophobicity of fluorine-containing epoxy resin is not as good as that of the modified titanium dioxide particles. However, the mechanical properties of the coating are better than those of the coating without fluorine-containing epoxy resin (B1).

When the mass ratio of fluorine-containing epoxy resin (FEP) and titanium dioxide particles is 2:3 and 3:3, as shown in Fig. 7e–h, the titanium dioxide particles are almost covered by epoxy resin. The coating has large cavities and protrusions, most of which are in the tens of microns. The contact angle of oil is small, but the mechanical properties of the coating are good.

The chemical composition of the surface of B2 coating was analyzed by EDS and XPS (see Fig. 8). It was shown that that the B2 coating contains C, O, F, Ti, Si elements, and these elements are uniformly distributed on the surface. The F element content of coatings cured with F-D400 is higher than that of D400 cured coatings (the composition is the same as that of B2 coating), indicating that fluoroepoxy (FEP) enhances the oleophobicity of the coating.

Figure 8e shows the XPS total spectrum of B2 coating (fluorine-containing epoxy resin (FEP):

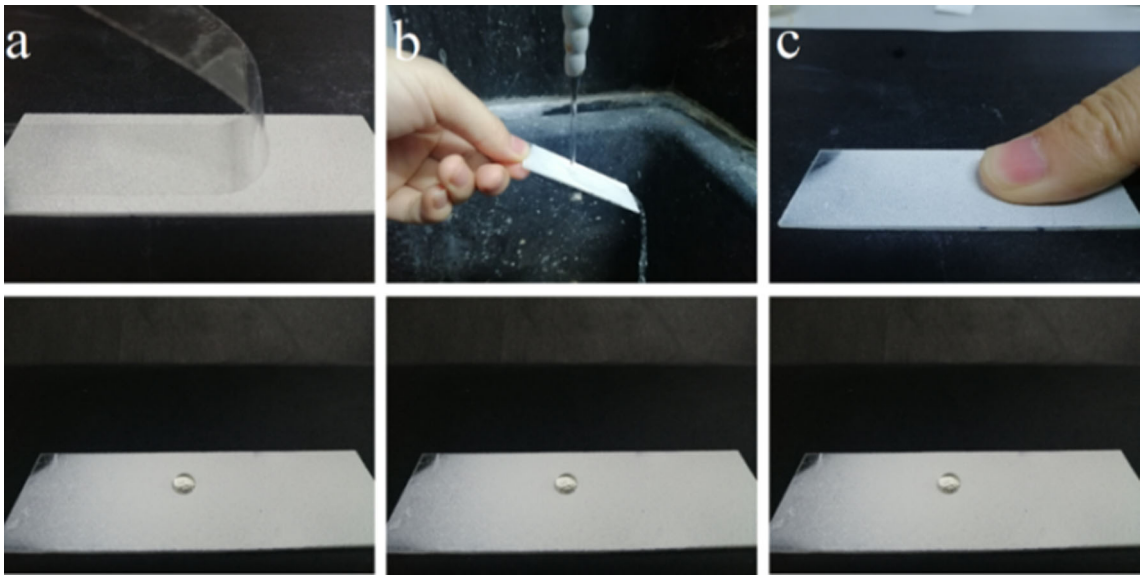

Figure 9 Coating stability test **a** tape peeling test, **b** water impact test, and **c** finger pressing test.

Table 3 Water contact angle of copper mesh after being soaked in solution for different time

Time (min)	0	0.5	1	5	7	10	20
WCA (°)	142.5 ± 1.3	100.6 ± 0.7	81.4 ± 1.2	0	0	0	0

modified titanium dioxide particles = 1:3), indicating the presence of C, O, F, Ti, and N elements. According to XPS data, it can be revealed that the proportions of C, O, F, Ti, and N are 57.4%, 19.99%, 17.43%, 1.31%, and 3.88%, respectively. Figure 8c is a high-resolution C1s spectrum, which is assigned to CF_3 (294.31 eV), CF_2 (291.96 eV), C=O (288.12 eV), C–O, C–N (286.40 eV), C–C, and C–H (284.8 eV) peak. Figure 7d is the high-resolution spectrum of F 1 s, in which two fitted peaks correspond to CF_3 (689.42 eV), CF_2 (688.58 eV).

It can be seen from the XPS spectrum that the content of F element on the surface of the superhydrophilic/superoleophobic coating B2 is 17.43%, being in the form of CF_2 and CF_3. The fluorine element is derived from perfluorooctanoic acid and fluorine-containing epoxy resin on the surface of titanium dioxide particles in the coating. At the same time, the content of Ti element on the surface of the coating is only 1.31%, indicating that the fluorine-containing epoxy resin covers most of the coating surface, resulting in excellent adhesive strength and mechanical property of the coating.

The mechanical stability of coating B2 was investigated by tape peeling, water rinsing, and finger pressing experiments (see Fig. 9). After 50 times of tape stripping, water rinsing (rinse time 1 h), and finger pressing experiments, the soybean oil drops are still spherical on the coating surface, and the contact angle is basically unchanged, showing the coating is still superhydrophilic and superoleophobic. Also, after the coating was placed outdoors for 60 d, the static contact angle of water is 0°, and that of soybean oil is 156°, which is the proof that the superhydrophilic/superoleophobic coating also has long-term stability.

Structure and properties of copper meshes coated with superhydrophilic/superoleophobic coatings (coating B2)

Wetting properties and structure of copper mesh

In order to obtain oil–water separation material with good comprehensive properties, multiply structural combination was utilized by spraying the coating B2 on the superhydrophilic copper mesh. Here, the optimal treatment for copper mesh is in demand. The copper mesh was soaked in solution, and soaking

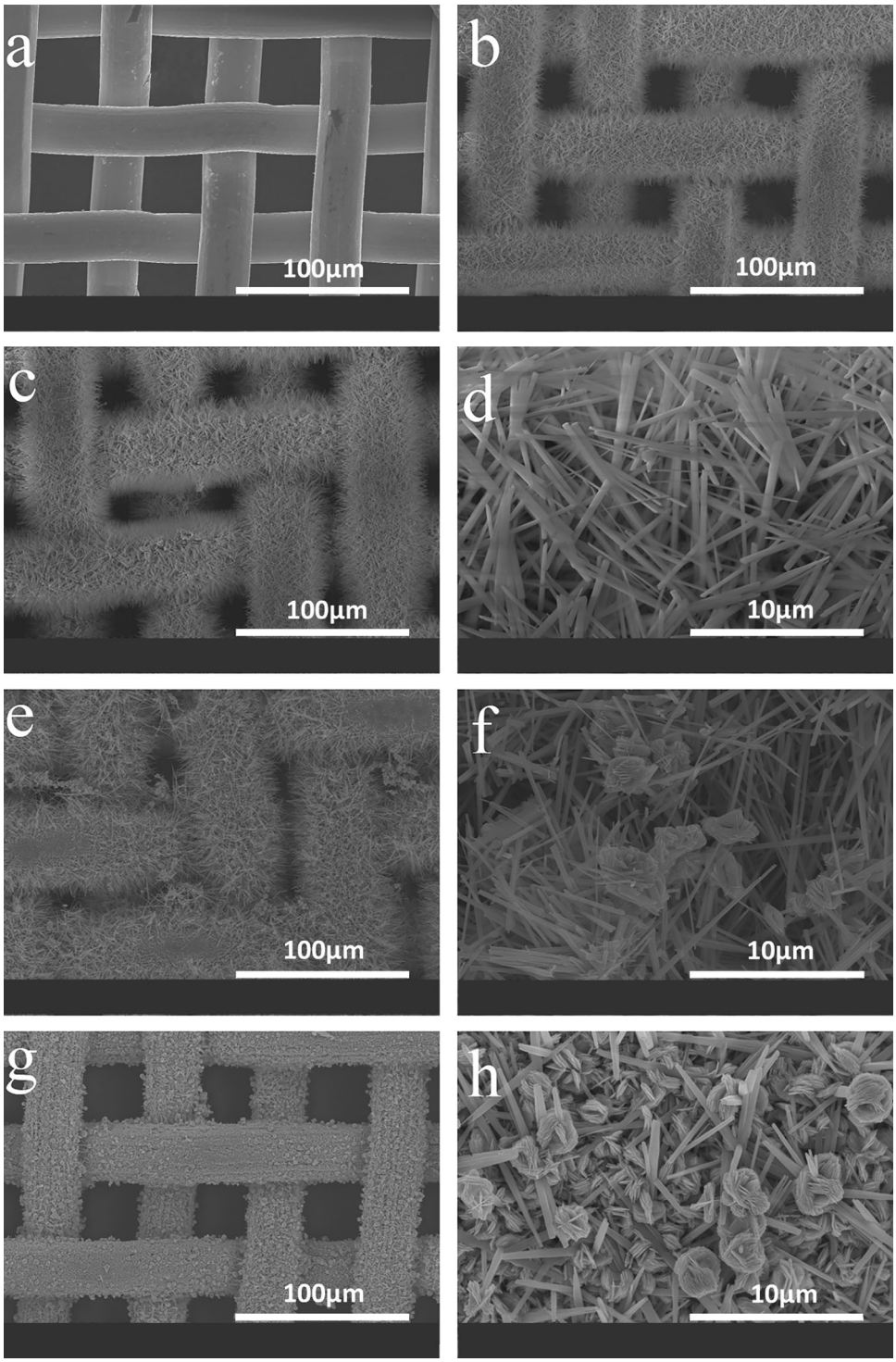

Figure 10 SEM images of copper mesh with different soaking time **a** original copper mesh, **b** soaking for 1 min, **c** and **d** soaking for 5 min, **e** and **f** soaking for 7 min, **g** and **h** soaking for 10 min.

time has an effect on the wetting property of the copper mesh. The water contact angle of the soaked copper mesh is shown in Table 3. The original copper mesh is hydrophobic (WCA: 142.5 ± 1.3°) with a pore size of about 30 μm. After being soaked in sodium hydroxide and ammonium persulfate for 0.5 min, WCA of the copper mesh is down to 100.6 ± 0.7°; being soaked for 1 min, the copper mesh is hydrophilic, and WCA was 81.4 ± 1.2°; when the time exceeds 5 min, the copper mesh becomes superhydrophilic, water can spread on the surface of

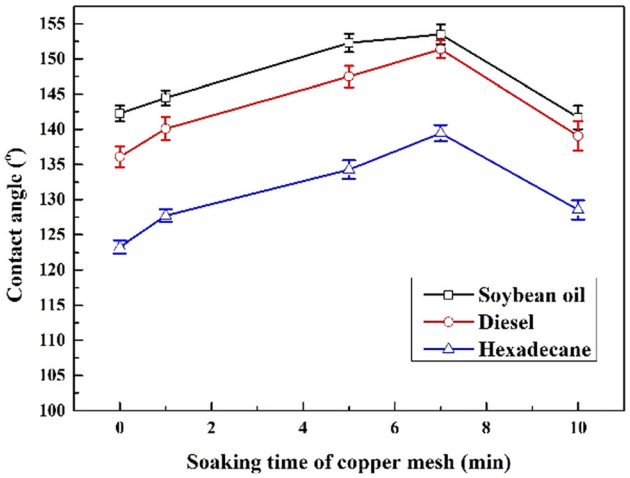

Figure 11 Effect of soaking time on contact angle of copper mesh coated by superhydrophilic/superoleophobic paint.

the copper mesh instantly, and the water contact angle is 0°.

Figure 10 shows the SEM images of copper mesh samples after soaking in NaOH and $(NH_4)_2S_2O_8$ aqueous solutions for (a) 0 min, (b) 1 min, (c and d) 5 min, (e–f) 7 min, (g-h) 10 min. After being soaked in alkaline aqueous solution, the color of the copper mesh surface gradually changes to light blue, blue, dark blue to black with time. The surface of the copper mesh is rapidly oxidized to Cu^{2+} by the oxidant $(NH4)_2S_2O_8$, forming $Cu(OH)_2$ nanorod array, which gradually changes from hydrophobicity to hydrophilicity. The principle is shown in formula (4).

$$Cu + 4NaOH + (NH_4)_2S_2O_8 \rightarrow Cu(OH)_2 + 2Na_2SO_4 + 2NH_3 \uparrow + 2H_2O \quad (4)$$

As shown in Fig. 10a, the copper wire diameter and voids of the original 700-mesh copper mesh are about 30 μm, and the surface of the copper mesh is smooth and hydrophobic. After being soaked for 1 min, as shown in Fig. 10b, arrays of nanorods appeared on the surface of the copper mesh, making the diameter of the copper wires a little larger and the voids smaller. The surface of the copper mesh becomes rough and is hydrophilic. As shown in Fig. 10c and d, with the prolongation of soaking time, after being soaked for 5 min, the length of the surface nanorods exceeds 10 μm and the voids of the copper mesh become smaller, being superhydrophilic. After the copper mesh has been soaked for 7 min, as shown in Fig. 10e and f, the nanorod array almost completely blocked the original gap, and nano-flower was grown above the nanorod array, microflowers, and nanorod arrays form a layered structure. When the soaking time is up to 10 min, as shown in Fig. 10g–h, the nanorods gradually transformed into nano-micro-flowers, the length of the nanorods was reduced, and the diameter of the copper wire became similar to that of the original copper mesh. As the soaking time is varied, the copper mesh can be from intrinsic hydrophobicity → (oxidation and roughness increase) → intrinsic hydrophilicity → (continuously increasing roughness) → superhydrophilicity.

Structure and properties of copper meshes covered with B2 coating

The coating B2 was sprayed on the copper mesh with being soaked for 0, 1, 5, 7, and 10 min in the treatment solution to obtain oil–water separation materials. The change of the contact angle of oil–water separation material is shown in Fig. 11. When coating B2 was sprayed to the unsoaked copper mesh, the contact angles of the coating to water, soybean oil, diesel oil, and hexadecane were 0°, 142.3 ± 1.1°, 136.1 ± 1.5°, 123.3 ± 0.9°, respectively, slightly smaller than the contact angle sprayed on a glass slide. This is because the copper mesh has voids and the resulting surface coating is less dense than that on a glass slide. When B2 coating was sprayed onto the copper mesh that had been soaked for 1, 5, and 7 min, the contact angles of soybean oil, diesel oil, and hexadecane on the copper mesh are gradually larger due to the increase in the roughness of the copper mesh.

When sprayed to the copper mesh with the treatment time of 7 min, the contact angles of water, soybean oil, diesel oil, and hexadecane on the copper mesh are 0°, 153.5 ± 1.4°, 151.4 ± 1.2°, and 139.5 ± 1.2°, respectively. Since the nanorods on the surface of the copper mesh are almost fluffy at this time, the surface roughness of the coating can be improved, resulting in high oleophobicity. When sprayed onto the copper mesh soaked for 10 min, the contact angle becomes smaller again.

Figure 12 is SEM images of copper mesh coated with coating B2, in which the copper mesh was soaked for 0, 1, 5, 7, and 10 min. As shown in Fig. 12a and b (the coating is sprayed on the original copper mesh), the copper mesh itself has large voids, and the copper wire in mesh is covered by the paint. During the process of oil–water separation, oil is easy to

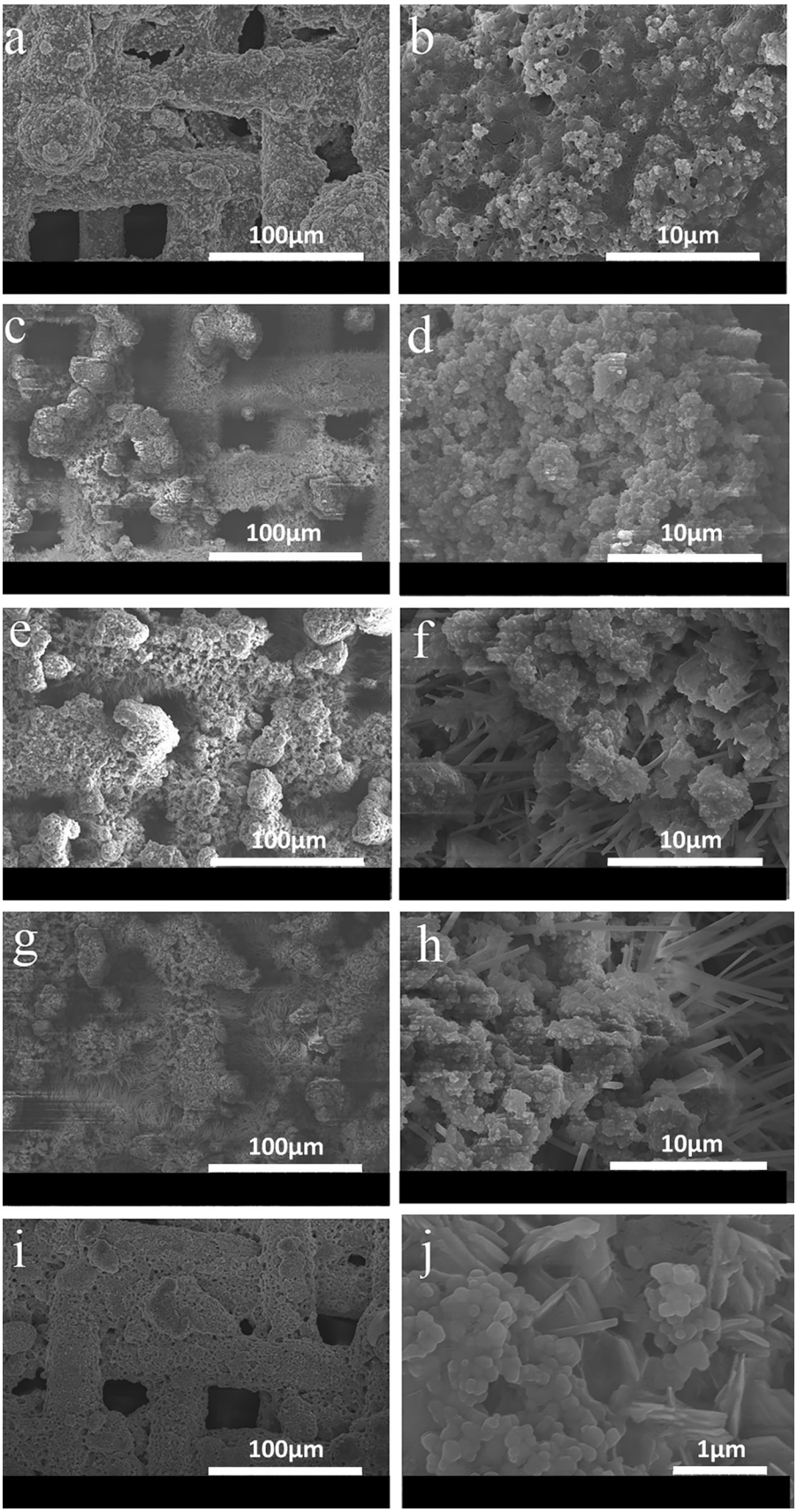
a
100μm
b
10μm
c
100μm
d
10μm
e
100μm
f
10μm
g
100μm
h
10μm
i
100μm
j
1μm

◀**Figure 12** SEM images of copper mesh coated with superhydrophilic/superoleophobic coating B2, in which the copper mesh was soaked for 0, 1, 5, 7, and 10 min. **a**, **b** 0 min, **c**, **d** 1 min, **e**, **f** 5 min, **g**, **h** 7 min, **i**, **j** 10 min.

filtrate from the large voids, resulting in low separation efficiency. In Fig. 12c and d (coating B2 was sprayed on the copper mesh soaked for 1 min), the copper mesh gap is still large, and the coating sprayed on the surface can cover the nanorods. From Fig. 12e and f (coating B2 was sprayed on the copper mesh soaked for 5 min), the nanorod array of the copper mesh is dense enough and the void is small; the sprayed coating solution can mostly stay on the copper mesh; some rods are also long enough to be exposed on the surface of the coating. When coating B2 was sprayed on the copper mesh soaked for 7 min, its structure was shown in Fig. 12g and h, the copper mesh gap was basically covered by nanorods, and the structure was fluffy. According to the Wenzel model, the increase in the roughness of surface can increase its wettability, and the existence of nanorod arrays enhances the superhydrophilic/superoleophobic properties of the coating to a certain extent. In the process of oil–water separation, when water passes through the coating surface, the nanorod array exposed on the coating surface can form a siphon effect, so that the water can pass through quickly, thereby the increase in water flux. SEM image of coating B2 on the copper mesh soaked for 10 min is shown in Fig. 12i and j. Most of the nanorod arrays on the surface of the copper mesh become nano-micro-flowers composed of nanosheets. The coating sprayed onto the surface of the copper mesh will cover most of the nanoflowers, the diameter of the copper wire also becomes similar to the diameter of the original unsoaked copper mesh, and voids appear. The coating cannot completely cover the surface after spraying, nor can it block the passage of oil well in the application of oil–water separation.

Application of coating

As shown in Fig. 13, the above optimal copper mesh coated by coating B2 was chosen as the oil–water separation material, and placed in the separator, clamped with a clamp. Pour 100 mL of water and 100 mL of the oil-insoluble mixture over the device. The water is able to penetrate the separation material very quickly, and the oil is left on top of the separation material, in which the separation process is driven only by gravity.

Mixtures of various oils (soybean oil, diesel, cetane, castor oil, olive oil, and sesame oil) with water were poured in the device to evaluate the oil–water separation efficiency. As shown in Fig. 14a and b, the separation efficiency of all oils was higher than 99.7%, and the water flux was higher than 80,000 L m^{-2} h^{-1}, and the highest was 91,719 L m^{-2} h^{-1}. This

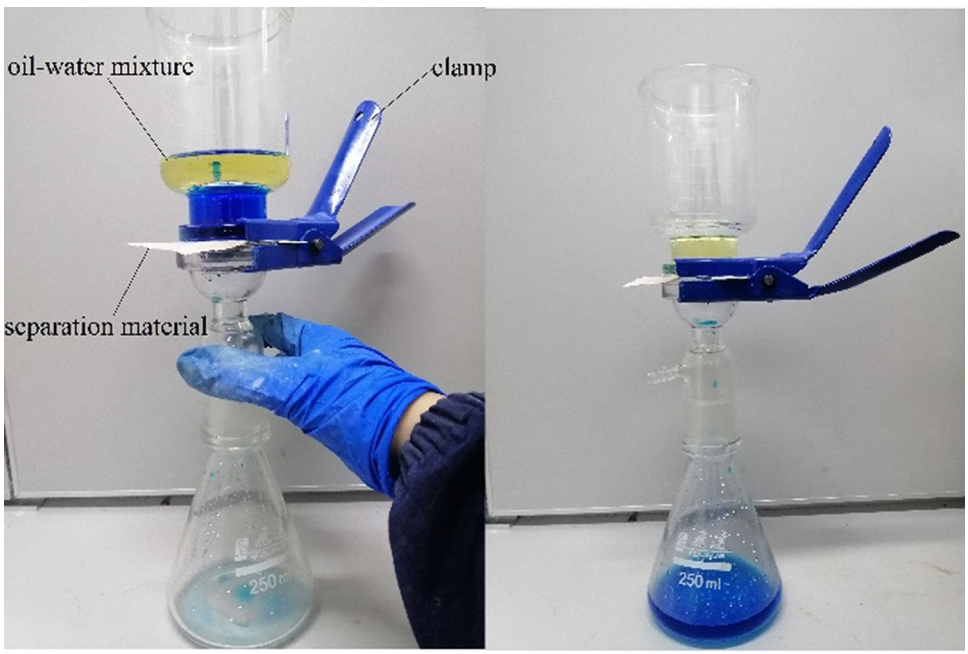

Figure 13 Oil–water separation device diagram.

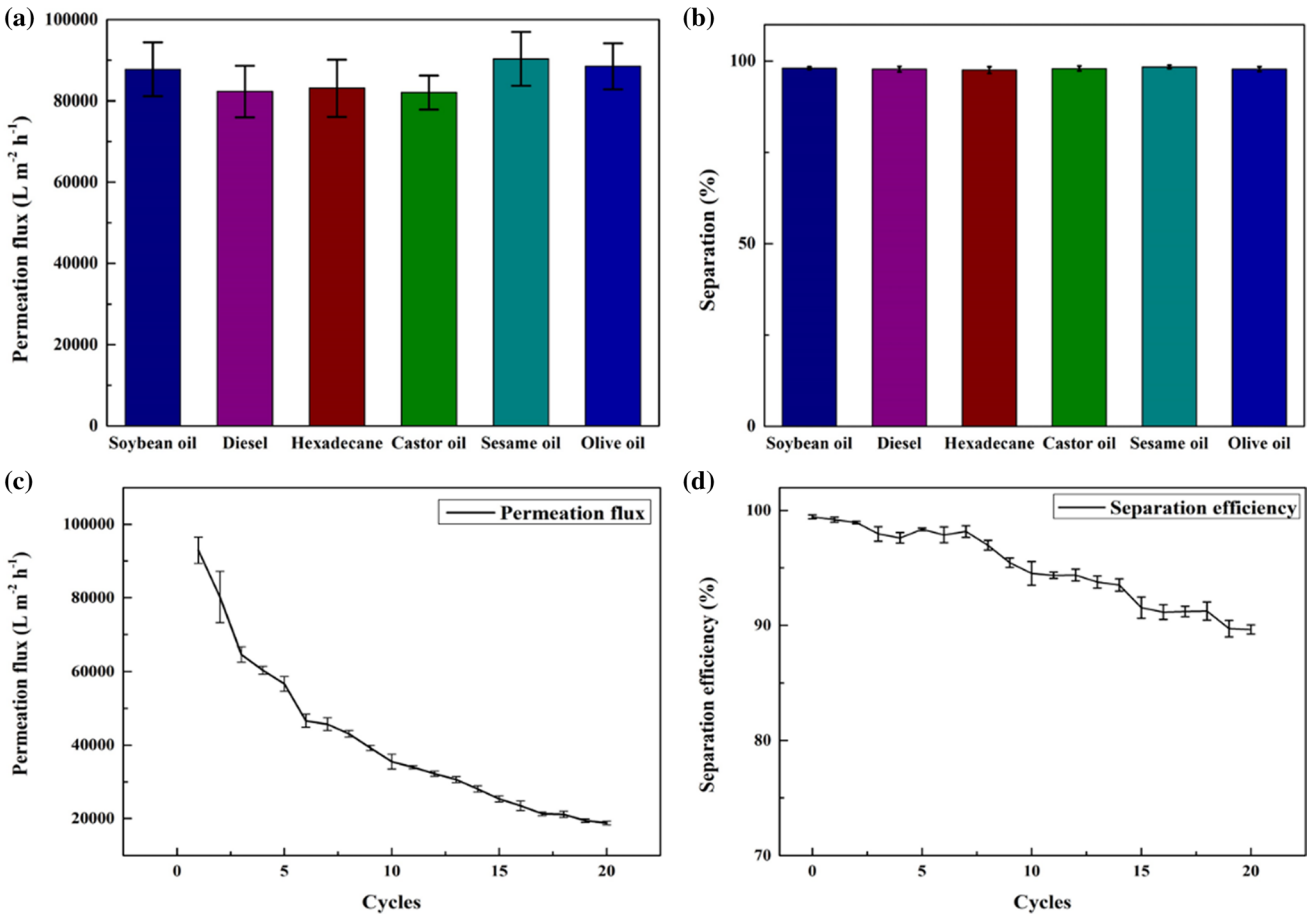

Figure 14 **a** Water separation flux of different oil–water mixtures, **b** separation efficiency of different oil–water mixtures, **c** separation efficiency change of water separation times, and **d** variation of water flux with separation times.

is because the nanorod array on the surface of the copper mesh by immersing for 7 min is exposed on the surface of the coating, which enhances the hydrophilicity of the surface, and the water is instantly wetted when it contacts the surface of the coating, and the siphon effect of the columnar nanorods can also make the water pass quickly. As shown in Fig. 14c and d, after 20 cycles, the separation efficiency is still higher than 90%, and the water flux is still 18,343 L m^{-2} h^{-1}, which has excellent oil–water separation ability. In this work, a superhydrophilic separation substrate was composited with a superhydrophilic/superoleophobic coating to prepare a separation material with high oil–water separation ability, whose separation water flux and separation efficiency are superior to some previous studies [21, 29, 30].

Conclusion

We have used perfluorooctanoic acid and polyetheramine to prepare fluorine-containing polyetheramine curing agent, which was cured with epoxy monomer to prepare fluorine-containing epoxy resin (FEP), and then mixed with superhydrophilic/superoleophobic titanium dioxide particles to prepare coating suspension. The oil–water separation material was prepared by spraying on the superhydrophilic copper mesh with rough structure. The superhydrophilic/superoleophobic supension containing fluorine-containing epoxy resin (FEP) and titanium dioxide particles with a mass ratio of 1: 3 was sprayed onto the copper mesh soaked for 7 min to prepare the oil–water separation material with the best comprehensive performance. The contact angles of soybean oil, diesel oil, and hexadecane on the surface of the oil–water material are 0°, 153.5 ± 1.4°,

151.4 ± 1.2°, 139.5 ± 1.2°, respectively. The separation efficiency of oil was higher than 99.7%, and the water flux was higher than 80,000 L m^{-2} h^{-1}, and the highest was 91,719 L m^{-2} h^{-1}. After 20 consecutive cycles, the separation efficiency was still higher than 90%, and the water flux was still 18,343 L m^{-2} h^{-1}, showing excellent oil–water separation capacity.

Acknowledgements

The authors acknowledge the financial support from East China University of Science and Technology.

Author contributions

RL contributed to writing—original draft, investigation, and data curation. RY contributed to conceptualization, funding acquisition, writing—review and editing. JF contributed to writing—review and editing. BC contributed to writing—review and editing.

Data availability

Data sharing is not applicable to this article.

Declarations

Competing interest The authors declare that they have no known competing financial interests or personal relationships that could have appeared to influence the work reported in this paper.

References

[1] Ge J, Shi LA, Wang YC, Zhao HY, Yao HB, Zhu YB, Zhang Y, Zhu HW, Wu HA, Yu SH (2017) Joule-heated graphene-wrapped sponge enables fast clean-up of viscous crude-oil spill. Nat Nanotechnol 12:434–440. https://doi.org/10.1038/nnano.2017.33

[2] Bolisetty S, Peydayesh M, Mezzenga R (2019) Sustainable technologies for water purification from heavy metals: review and analysis. Chem Soc Rev 48:463–487. https://doi.org/10.1039/c8cs00493e

[3] Zeng Y, Yang C, Zhang J, Pu W (2007) Feasibility investigation of oily wastewater treatment by combination of zinc and PAM in coagulation/flocculation. J Hazard Mater 147:991–996. https://doi.org/10.1016/j.jhazmat.2007.01.129

[4] Painmanakul P, Sastaravet P, Lersjintanakarn S, Khaodhiar S (2010) Effect of bubble hydrodynamic and chemical dosage on treatment of oily wastewater by induced air flotation (IAF) process. Chem Eng Res Des 88:693–702. https://doi.org/10.1016/j.cherd.2009.10.009

[5] Liu J, Wang L, Guo F, Hou L, Chen Y, Liu J, Wang N, Zhao Y, Jiang L (2016) Opposite and complementary: a superhydrophobic–superhydrophilic integrated system for high-flux, high-efficiency and continuous oil/water separation. J Mater Chem A 4:4365–4370. https://doi.org/10.1039/c5ta10472f

[6] Gupta RK, Dunderdale GJ, England MW, Hozumi A (2017) Oil/water separation techniques: a review of recent progresses and future directions. J Mater Chem A 5:16025–16058. https://doi.org/10.1039/c7ta02070h

[7] Wang F, Lei S, Xue M, Ou J, Li W (2014) In situ separation and collection of oil from water surface via a novel superoleophilic and superhydrophobic oil containment boom. Langmuir 30:1281–1289. https://doi.org/10.1021/la403778e

[8] Shayesteh H, Rahbar-Kelishami A, Norouzbeigi R (2022) Superhydrophobic/superoleophilic micro/nanostructure nickel particles for oil/water mixture and emulsion separation. Ceram Int 48:10999–11008. https://doi.org/10.1016/j.ceramint.2021.12.320

[9] Zhou L, Su C, Chen B, Zhao Q, Wang X, Zhao X, Ju G (2022) Durable ER@SiO_2@PDMS superhydrophobic composite designed by double crosslinking strategy for efficient oil-water separation. Polymer 245:124722. https://doi.org/10.1016/j.polymer.2022.124722

[10] Feng L, Zhang Z, Mai Z, Ma Y, Liu B, Jiang L, Zhu D (2004) A superhydrophobic and superoleophilic coating mesh film for the separation of oil and water. Angew Chem-Int Edit 43:2012–2014. https://doi.org/10.1002/anie.200353381

[11] Li J, Kang R, Tang X, She H, Yang Y, Zha F (2016) Superhydrophobic meshes that can repel hot water and strong corrosive liquids used for efficient gravity-driven oil/water separation. Nanoscale 8:7638–7645. https://doi.org/10.1039/c6nr01298a

[12] Matsubayashi T, Tenjimbayashi M, Komine M, Manabe K, Shiratori S (2017) Bioinspired hydrogel-coated mesh with superhydrophilicity and underwater superoleophobicity for efficient and ultrafast oil/water separation in harsh environments. Ind Eng Chem Res 56:7080–7085. https://doi.org/10.1021/acs.iecr.7b01619

[13] Yang J, Yu T, Wang Z, Li S, Wang L (2022) Substrate-independent multifunctional nanostructured coating for diverse wastewater treatment. J Membr Sci 654:120562. https://doi.org/10.1016/j.memsci.2022.120562

[14] Wang M, Hu DD, Li YD, Peng HQ, Zeng JB (2022) Bio-based mussel-inspired underwater superoleophobic chitosan

derived complex hydrogel coated cotton fabric for oil/water separation. Int J Biol Macromol 209(Pt A):279–289. https://doi.org/10.1016/j.ijbiomac.2022.04.007

[15] Ni T, You Y, Xie Z, Kong L, Newman B, Henderson L, Zhao S (2022) Waste-derived carbon fiber membrane with hierarchical structures for enhanced oil-in-water emulsion separation: Performance and mechanisms. J Membr Sci 653:120543. https://doi.org/10.1016/j.memsci.2022.120543

[16] Qu M, He D, Luo Z, Wang R, Shi F, Pang Y, Sun W, Peng L, He J (2022) Facile preparation of a multifunctional superhydrophilic PVDF membrane for highly efficient organic dyes and heavy metal ions adsorption and oil/water emulsions separation. Colloids Surf A 637:128231. https://doi.org/10.1016/j.colsurfa.2021.128231

[17] Zhou Y, Zuo J, Zhao T, Chen Z, Chen M, Xu S, Cheng J, Wen X, Pi P (2022) A durable biomimetic superhydrophilic/underwater superoleophobic fabric bed for highly efficient emulsion separation. Mater Today Commun 31:103561. https://doi.org/10.1016/j.mtcomm.2022.103561

[18] Zeng Z, Wu X, Liu Y, Chen C, Tian D, He Y, Wang L, Yang G, Zhang X, Zhang Y (2022) Fabrication of a durable coral-like superhydrophilic MgO coating on stainless steel mesh for efficient oil/water separation. Chem Eng Sci 248:117144. https://doi.org/10.1016/j.ces.2021.117144

[19] Yang J, Zhang Z, Xu X, Zhu X, Men X, Zhou X (2012) Superhydrophilic-superoleophobic coatings. J Mater Chem 22:2834–2837. https://doi.org/10.1039/c2jm15987b

[20] Yang J, Yin L, Tang H, Song H, Gao X, Liang K, Li C (2015) Polyelectrolyte-fluorosurfactant complex-based meshes with superhydrophilicity and superoleophobicity for oil/water separation. Chem Eng J 268:245–250. https://doi.org/10.1016/j.cej.2015.01.073

[21] Li F, Kong W, Zhao X, Pan Y (2020) Multifunctional TiO_2-based superoleophobic/superhydrophilic coating for oil–Water separation and oil purification. ACS Appl Mater Interfaces 12:18074–18083. https://doi.org/10.1021/acsami.9b22625

[22] Lu J, Zhu X, Miao X, Song Y, Liu L, Ren G, Li X (2020) Photocatalytically active superhydrophilic/superoleophobic coating. ACS Omega 5:11448–11454. https://doi.org/10.1021/acsomega.0c00474

[23] Lu G, Shuai C, Liu Y, Yang X, Hu X (2021) Design and preparation of PU/EP blend resin grafted by hydrophilic molecular segments. Coatings 11:1345. https://doi.org/10.3390/coatings11111345

[24] Qian Y, Zhang D, Cheng Z, Kang H (2018) Preparation of hydrophilic epoxy resin and its wettability regulation. Chem J Chin Univ-Chin 39:1823–1828

[25] Ying L, Peng S, Zhang X, Zhao W, Wu X (2012) Preparation and characterization of a fluorinated epoxy resin with hydrophilicity and oleophobicty. Paint Coat Ind 42:11–15+18

[26] Li W, Wu G, Tan J, Yu X, Sun G, You B (2019) Transparent surfactant/epoxy composite coatings with self-healing and superhydrophilic properties. Macromol Mater Eng 304:1800765. https://doi.org/10.1002/mame.201800765

[27] Qu M, Ma L, Zhou Y, Zhao Y, Wang J, Zhang Y, Zhu X, Liu X, He J (2018) Durable and recyclable superhydrophilic-superoleophobic materials for efficient oil/water separation and water-soluble dyes removal. ACS Appl Nano Mater 1:5197–5209. https://doi.org/10.1021/acsanm.8b01249

[28] Miccio LA, Fasce DP, Schreiner WH, Montemartini PE, Oyanguren PA (2010) Influence of fluorinated acids bonding on surface properties of crosslinked epoxy-based polymers. Eur Polym J 46:744–753. https://doi.org/10.1016/j.eurpolymj.2010.01.001

[29] Li F, Wang Z, Huang S, Pan Y, Zhao X (2018) Flexible, durable, and unconditioned superoleophobic/superhydrophilic surfaces for controllable transport and oil-water separation. Adv Funct Mater 28:1706867. https://doi.org/10.1002/adfm.201706867

[30] Sun Y, Guo Z (2020) Novel and cutting-edge applications for a solvent-responsive superoleophobic-superhydrophilic surface: Water-infused omniphobic surface and separating organic liquid mixtures. Chem Eng J 381:122629. https://doi.org/10.1016/j.cej.2019.122629